Urban Forestry & Urban Greening 121 (2026) 129470

Contents lists available at ScienceDirect

Urban Forestry & Urban Greening

journal homepage: www.elsevier.com/locate/ufug

Original article

Urban trees and structure loss in the 2025 Eaton and Palisades fires

Reed Kenny [a,*], Jason Johns [a], Camille Pawlak [a], Andrew Fricker [b], Jenn Yost [c], Matt Ritter [c]

[a] Urban Forest Institute, 1352 Pacific Ave, San Luis Obispo, CA 93402, United States
[b] Department of Social Sciences, California Polytechnic Institute San Luis Obispo, CA, United States
[c] Department of Biological Sciences, California Polytechnic Institute San Luis Obispo, CA, United States

ARTICLE INFO

Keywords:
Defensible space
Urban conflagration
Zone zero
Urban canopy cover

ABSTRACT

Wind driven, urban fires in California have increasingly produced large scale structure loss driven by ember exposure and rapid house to house spread. However, the relative influence of structure density, urban canopy, and near structure vegetation during urban conflagrations remains poorly understood. Here, we analyzed patterns of structure loss using CAL FIRE damage assessments, building footprint data, and high-resolution mapping of urban canopy and land cover, following two fires that burned through the southern California communities of Altadena and Pacific Palisades under extreme weather and wind conditions in 2025.

Across both fires, structure density was the strongest predictor of structure loss, increasing the probability of loss by 1.6 and 1.5 %age points (pp) per additional structure per hectare in the Eaton and Palisades fires, respectively. Canopy density exhibited contrasting associations, with higher canopy density associated with increased loss probability in the Eaton fire (+0.6 pp per canopy per hectare) but reduced loss probability in the Palisades fire (–0.24 pp per canopy per hectare). Using our model to simulate the removal of all canopy within two meters of a structure, slightly lowers the probability of loss relative to the average condition (3.4 pp for Eaton and 1 pp for Palisades).

Our results have important implications for urban forest management. They show that during large urban conflagrations, patterns of building density and arrangement play a far greater role in structure loss than the spatial distribution of urban vegetation. The small and inconsistent association of vegetation with structure loss observed in this study suggests that policies calling for the removal of urban canopy should be approached with caution and supported by further research.

1. Introduction

The impact and devastation of wildfires is increasing in the Western United States (Abatzoglou et al., 2021; Syphard and Keeley, 2020). In 2017 and 2018, California experienced the costliest fire seasons in the US to date with $148.5 billion in estimated damage. In 2018 alone, more than 20,000 structures were destroyed by wildfire (Wang et al., 2021). Many of the most destructive fires occur when wind driven wildfires burn into urban areas and turn into urban conflagrations (Price et al., 2025; Quarles et al., 2010). In January of 2025, two major fires burned from wildlands into the communities of Altadena and Pacific Palisades (the Eaton and Palisades fires), destroying 9413 and 6831 structures respectively (CalFire DINS data).

When extreme wind driven wildfires spread into communities and become urban conflagrations, embers typically ignite structures far ahead of the fire front, suppression is extremely difficult, and a majority of the structures are typically destroyed (Escobedo et al., 2024; Knapp et al., 2021; Troy et al., 2022). Prior work has found that in these urban conflagrations, structure loss is more likely in areas of higher building density (Knapp et al., 2021; Penman et al., 2019; Price and Bradstock, 2013; Zamanialaei et al., 2025). In these contexts, the structures themselves become the dominant fuel source and structure ignition drives the spread of the fire (Filkov et al., 2023). In addition to the role of structures themselves, it is important to understand whether other factors such as urban vegetation also contribute to structure loss.

Policies such as California's AB 3074 mandate the creation of an ember resistant zone within 5 ft of a structure (zone zero), which may include removal of all vegetation within that zone (CalFire, 2025). Application of these regulations in urban areas is built on the premise that vegetation such as urban trees and shrubs contributes significantly to structure loss in urban conflagrations. Urban trees and shrubs constitute the vast majority of plant biomass in cities and are critical

* Corresponding author.
E-mail address: rekenny@calpoly.edu (R. Kenny).

https://doi.org/10.1016/j.ufug.2026.129470
Received 30 December 2025; Received in revised form 21 April 2026; Accepted 23 April 2026
Available online 24 April 2026

assets, providing shade, reducing stormwater runoff, and enhancing aesthetic value (Davies et al., 2011; Giacinto et al., 2021; Pataki et al., 2021). An analysis by the LA county planning department calculated that on average 3.57% of the woody canopy cover of incorporated areas in LA county is within 5 ft of a structure (0.9% for unincorporated communities), a significant amount given California's goal of increasing urban canopy cover by 10% by 2035 (CA Assembly Bill 2251), (LA County DRP GIS Section, 2025). Given the substantial loss to urban canopy posed by this policy, it is critical to understand the role of urban vegetation in these fires, and whether its contribution is significant compared to other sources, such as structure-to-structure spread.

Structures and woody vegetation represent the majority of flammable material in urban areas, as both are principally made of wood. Notably, the wood in houses is milled and dried, whereas the wood in trees and shrubs is mostly saturated with water (Ehleringer and Dawson, 1992). While many urban trees and shrubs are widely spaced, pruned of dead material, and shaped to have canopies clear of the ground, they require maintenance to remove dry, flammable tissue such as dead leaves and branches (Barkeley et al., 2004; Speak and Salbitano, 2023). Further, urban tree irrigation and maintenance practices vary widely among municipalities (Bijoor et al., 2012; Speak and Salbitano, 2023). These factors all likely impact the role of urban vegetation on structure damage in urban fires, however, this has yet to be tested (Zhang et al., 2025).

Here, we investigated the association between urban vegetation and structure loss in the Eaton and Palisades fires and compared this to other factors such as structure density, wind speed and wind direction. To this end, we used a dataset of tree and shrub canopies derived from LiDAR and satellite imagery, as well as maps of structure footprints for Los Angeles County from the LARIAC program (LA Internal Services Department, 2020). We then combined this data with CAL FIRE's Damage Inspection (DINS) dataset, which assesses fire-caused structure damage. We used this combined dataset to evaluate and compare factors contributing to structure damage in these fires, including structure density, vegetation density, and defensible space in zone zero, as well as variables related to ember and flame exposure such as wind direction and the distance and bearing to the nearest structure and vegetation. Although the wind and weather conditions in these fires were extreme, these are exactly the conditions that ember resistant zones and home hardening are designed to mitigate (Guirguis et al. 2025). Investigating the relationship between structure damage and the above variables during such extreme conditions should thus provide information relevant to the worst-case scenario events that regulatory actions are designed to mitigate against. In more moderate fire conditions fire suppression is generally effective, and it is unlikely for a fire to burn into an urban area or generate the ember showers that are so dangerous (Syphard et al. 2022). Scientifically examining the rationale for implementing vegetation control in fire-prone urban areas is especially important given the potential impact to communities and the politically charged nature of the questions. We interpret our results as urban forestry researchers; however, we believe the value in this work comes from sharing the results publicly to allow for a plurality of interpretations.

2. Methods

2.1. Study areas

Our study area was bounded by the final fire perimeters of the Eaton and Palisades fires as determined by CAL FIRE (National Interagency Fire Perimeters, 2025). Because mapped burn perimeters do not represent strict physical boundaries (e.g., some structures outside the perimeter may be burned, and others within may remain unburned) we restricted all analyses to a 50 m buffer interior to the final burn perimeters to reduce edge-related bias. Within this final perimeter, we only examined vegetation up to 50 m from structures that may have been affected by the fires. Our analysis focused on sections of the burned area where neighborhoods experienced relatively uniform fire severity. We excluded urban areas to the west of Pacific Palisades where the fire burned patchily through only some neighborhoods as well as areas to the east of Altadena where the fire only burned slightly past the wildland-urban interface. Our final study areas are shown in Fig. 1.

2.2. Datasets

We compiled a remote sensing dataset that included pre-fire LiDAR and multispectral imagery. Pre-fire LiDAR was obtained from the Los Angeles Region Imagery Acquisition Consortium (LARIAC) program (collected 2023–24) and has a nominal point density of 2 points per m^2 (County of Los Angeles, 2025). We also obtained pre-fire Maxar satellite imagery (Maxar Technologies Inc., Westminster C.O., US) with the following specifications: 8-band imagery at 1.4 m resolution, panchromatic imagery at

35 cm resolution, and 3-band Red Green Blue (RGB) imagery also at 35 cm resolution. Maxar imagery dates were October 20, 2024 (Palisades), and January 1, 2025 (Eaton).

To assess structure loss, we used data from the CALFIRE Damage Inspection (DINS) program, which documents post-fire structure damage. To create a binary response variable, we grouped structures classified as "no damage" or "affected" (1–9% damaged) into "not destroyed" and structures classified as "minor damage" (10–25% damaged), "major damage" (26–50% damaged), or "destroyed" (>50% damaged) as "destroyed". We also used the 2020 LARIAC structure footprints dataset for LA County to delineate structure footprints (LA Internal Services Department, 2020).

2.3. Geospatial analyses

2.3.1. Preparation of point cloud data

In order to create a map of the location of urban vegetation before the fires, we first used our pre-fire LiDAR data to create a model representing the height and shape of all tree and shrub canopies as well as buildings. To do this, pre-fire LiDAR point cloud data were processed using the R package *lidR* (Roussel et al., 2020). Classified ground points were used to normalize non-ground returns so that non-ground returns reflect the heights of the vegetation or buildings relative to the ground. We classified noise using the *classify_noise* function. We then removed returns identified as noise, along with those below 0 or greater than 150 ft (45.72 m) above ground level. A pit-free smoothed canopy height model (CHM) was then generated using a triangulation method.

2.3.2. Alignment of LiDAR and satellite imagery

In order to use both LiDAR and satellite imagery to map the location of urban canopy, we had to ensure that the layers were adequately aligned with each other. Misalignments between datasets acquired at different times or with different sensors can introduce substantial error in spatial analyses (Brigham et al., 2024). To align them, we developed a custom Python script to co-register LiDAR and satellite imagery layers. The LiDAR-derived canopy height model was first resampled to match the spatial resolution of the one-band (panchromatic) Maxar imagery. Values of both layers were then normalized to between 0 and 1. This results in two black and white images, one representing elevations (LiDAR) and one representing reflectance (satellite). The images were similar enough that we were able to align them using phase cross correlation, a method that detects mismatches in patterns at the pixel level and is robust to differences in brightness. We implemented phase cross correlation using the scikit-image library and the phase_cross_correlation function (Van Der Walt et al., 2014) thereby aligning our LiDAR and satellite data. Accuracy of the alignment was assessed using 40 points that could be identified in both the LiDAR and satellite images. Root mean squared error of the Euclidean distance between the matched points was calculated to estimate the average offset between images.

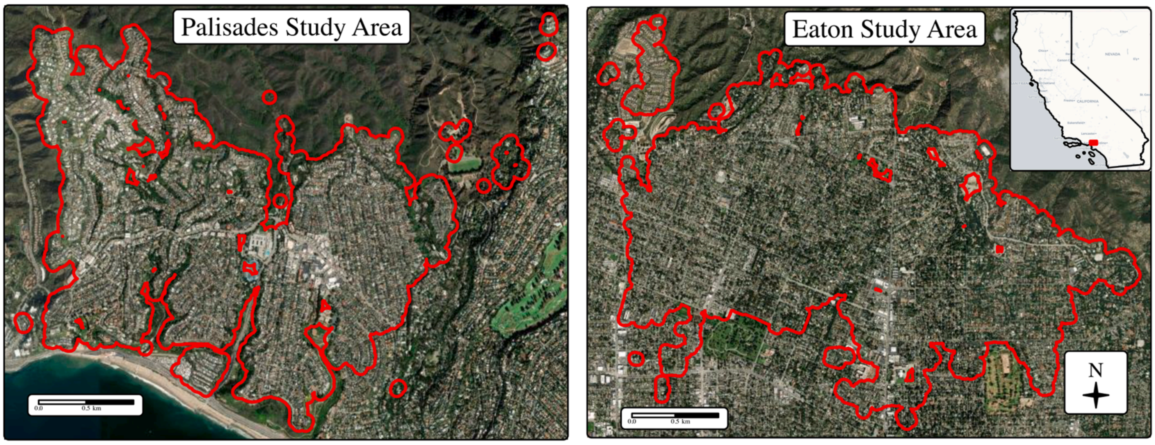

Fig. 1. Red outlines represent our study areas in Pacific Palisades, California (left) and Altadena, California (right), inset at the top shows location in California of both fires.

The custom scripts for this analysis can be found in the project Github repository below along with the other scripts for spatial analysis.

2.3.3. *Canopy segmentation*

Once our LiDAR and satellite data were aligned, we could use both of them together to map the boundaries of individual canopies in our study

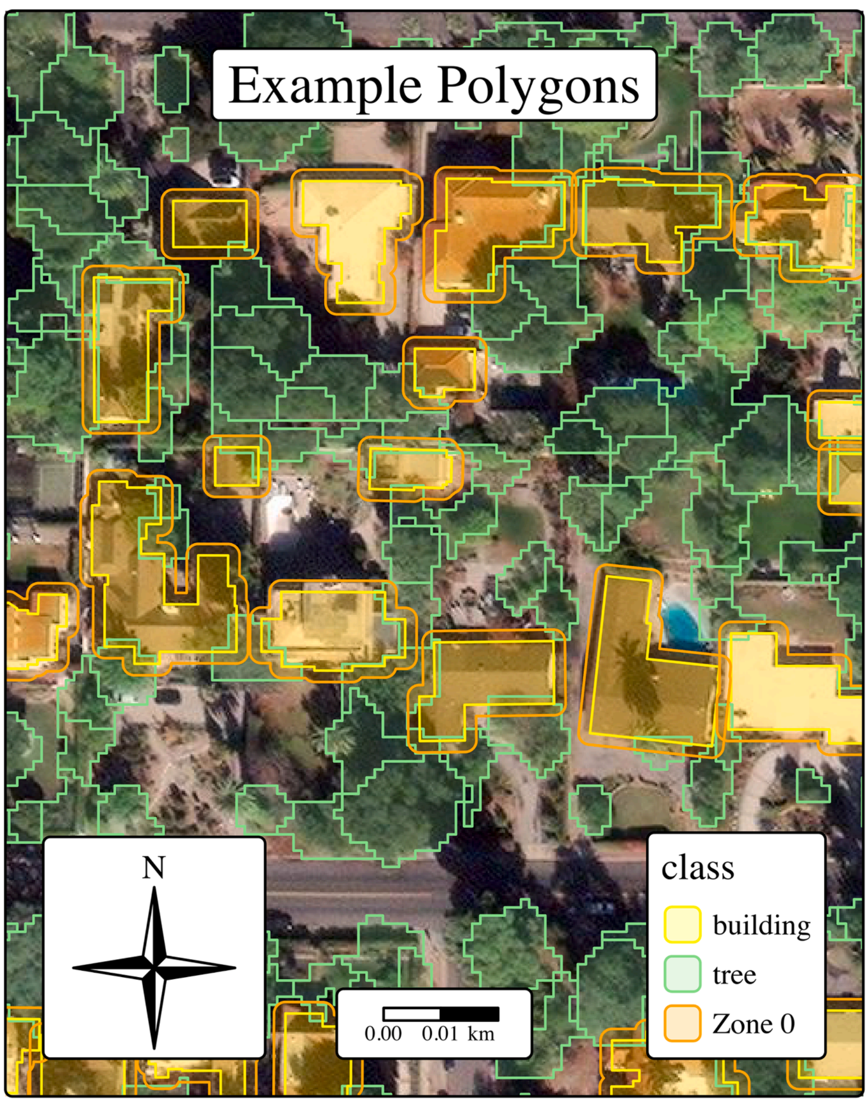

Fig. 2. Example tree crown and structure footprint polygons plotted on top of Maxar RGB imagery captured October 20, 2024. Orange lines show the two meter buffer around a structure in which we calculated the area of tree canopy as well as the area of other structures.

areas. Individual canopy polygons were segmented from the co-registered pre-fire canopy height model using the lidR package in R (Roussel et al., 2020). We applied the segmentation algorithm developed by Dalponte and Coomes (2016), which integrates local maxima filtering with a marker-controlled watershed approach (Dalponte and Coomes, 2016). We calculated local maxima using the locate_trees() function with a custom window size function defined as {x * 0.15 + 5} where x is the height of the pixel. These local maxima were used in the Dalponte and Coomes algorithm, along with the settings minimum tree size = 0.5 m and maximum crown diameter = 30 m.

The input for segmentation was the canopy height model derived from the pre-fire LiDAR, with structure footprints masked using the LARIAC buildings footprints layer to avoid interference from anthropogenic structures and a smoothing algorithm applied using the R package *terra* (Hijmans, 2025). Following segmentation, we filtered the resulting canopy polygons by vegetation index: polygons with a pre-fire Normalized Difference Vegetation Index (NDVI) below 0.5 (calculated from the pre-fire satellite imagery) were excluded from the final dataset. We chose 0.5 as a threshold to be conservative in only including live trees in the dataset, as live tree canopies have been found to have NDVI values between 0.45 and 0.6 (Hardy and Burgan, 1999). Example canopy polygons can be seen in Fig. 2.

The accuracy of our tree crown polygons was assessed using 500 randomly placed points stratified equally between canopy and non-canopy areas for each study site. We used our high resolution satellite imagery collected pre-fire (Eaton: Jan 1, 2025, Palisades: Oct 20, 2024) to determine whether our canopy model (canopy/non-canopy) corresponded to what we observed at each of our random points. We used the confusionMatrix function from the R package *caret* 7.0.1 to generate the confusion matrix and accuracy statistics (Kuhn, 2008).

2.4. Wind data

These fires, like most other highly destructive fires that begin in wildlands, happened during an extreme wind event. Wind direction and speed directly affect radiative exposure, convection, and ember deposition (Filkov et al., 2023). As such, we included wind direction and speed in our models. For each structure footprint in our study areas, we extracted the average wind direction and speed over the plausible burn window (Eaton 6:00 pm, Jan 7–11:00 am Jan 8, 2025: Palisades 11:00 am Jan 7–8:00 pm Jan 8). We modeled high resolution wind data using WindNinja (Wagenbrenner et al., 2024). For the Eaton fire we used data from the remote automated weather station at Henninger flats as input for the wind model. We modeled wind vectors across the study area for each hourly time step available from the weather station during the plausible burn window. Output wind speed and direction were at 60 m resolution and for each structure polygon we extracted the mean wind speed and direction experienced over the plausible burn window. For the Palisades fire we used wind data from NOAH's High Resolution Rapid Refresh (HRRR) atmospheric model at 10 m above ground level, at hour intervals during the above burn windows as input for WindNinja. We downloaded HRRR data using the python library *herbie* (Dowell et al., 2022). Output wind speed and direction were at 200 m resolution and we extracted mean wind speed and direction as above.

2.4.1. Spatial statistics

Within our study boundaries, we computed a set of spatial metrics for each structure. We calculated the distance and bearing to the nearest structure (structure separation distance), as well as distance and bearing to the edge of the nearest canopy. Similarly, we measured the total canopy area within 2 m of a structure. In the case that there was another structure within two meters of our focal structure, we also measured the area of that structure that was within the 2 m buffer (Fig. 2). We chose 2 m to roughly correspond with the inner zone (zone zero) of many defensible space regulations that potentially specify removal of all flammable materials within the zone immediately adjacent to a structure (5 ft) (CalFire, 2025; Nowicki, 2002). We calculated the area of canopy as well as the area of other structures to approximate the total amount of flammable material within the 2 m buffer zone. To assess whether a structure was downwind of the nearest canopy or structure, we calculated the angular difference between the bearing to the nearest canopy or structure and the mean wind direction. This may be significant as flame lengths and convective heating can be significantly different on the upwind vs downwind side of a burning structure or tree (Filkov et al., 2023). To create a metric where 0 represents directly downwind and 180 directly upwind, we calculated the angular difference as the smallest of the absolute value of the difference of the mean wind direction and the measured bearing, or 360 minus the absolute value of the difference of the mean wind direction and the measured bearing and refer to this as degrees from downwind.

We also quantified variation in canopy and structure densities across the study areas. Kernel density estimation can generate a smooth distribution representing the probability of occurrence of canopy or structures across the landscape, which can be scaled to a point density value. This is advantageous as information about the spacing between objects can be summarized over the entire area and so provide a more nuanced metric than just the distance to the closest canopy or structure. Because kernel bandwidth can have a large influence on the output, we tested kernel density bandwidths of 200 m, 300 m and 500 m. We computed kernel density estimates for both canopy and structure footprints using the R function *sf.kde* and the above kernel widths with the settings resolution = 30 m, standardize = FALSE and scale factor = 1. We then standardized the kernel density to output points per hectare and extracted the mean value at each structure polygon using the R package *terra.* This gives us a continuous measure of canopy or structure density across our study areas. From here on we refer to these metrics as structure density and canopy density. To account in part for topographic influences on fire behavior, we calculated the slope, aspect and elevation for each structure polygon using the R function terrain() in the *terra* package and included these as predictors in out models.

All spatial analyses were performed in R version 4.4.2 using the *sf* (v1.0.19) and *terra* (v1.8.21) packages (Hijmans, 2025; Pebesma and Bivand, 2023). Reproducible code is available at {redacted for review}, and raw data can be accessed at DOI: 10.5061/dryad.5hqbzkhkd.

2.5. Statistical analyses

We used spatially explicit generalized linear mixed-effects models (GLMMs) to explore the influence of canopy and structure spatial characteristics on the likelihood of structure loss. Each row in the input data for the model represented an individual structure and the spatial variables associated with that structure. Models were implemented using the *spaMM* package in R, incorporating spatial autocorrelation via the stochastic partial differential equation (SPDE) approach with a mesh maximum edge length of 200 m and fit using logistic regression with a logit-link function (Lindgren et al., 2011; Rousset, F. and Ferdy, J.-B., 2014). Though our response classes were somewhat unbalanced (76–79% destroyed, see Results), the number of outcome events and non-outcome events was large relative to model complexity. The limiting class represented greater than 100 events per fixed-effect parameter across both models. This is well above the commonly cited thresholds for reliable estimation in logistic regression and we therefore do not expect class imbalance to bias coefficient estimates (Peduzzi et al., 1996; Riley et al., 2019).

We conducted model selection to determine the optimum kernel width to use for our kernel density metrics. All candidate models included a spatial random intercept term as well as distance to the nearest structure, distance to the nearest canopy, area of canopy within 2 m, area of structure footprint within 2 m, degrees from downwind from the nearest structure and degrees from downwind from the nearest canopy and input data was scaled and centered. We tested all combinations of our three kernel widths applied to canopy density as well as structure density and chose those models with the lowest AIC scores. We also tested for significant interactions between canopy density and structure density, as well as the distance and degrees from downwind from the nearest canopy and the nearest structure. We retained interactions when they resulted in a delta AIC of two or greater, otherwise we chose the simpler model. We calculated covariance matrices for all tested models and rejected models containing predictors that had a higher correlation than 0.5 (Supp. Figs. 1 & 2).

We report as significant only predictors having estimates with 95% confidence intervals that did not overlap zero 0 (Wald t value > 1.96). We determined the relative importance of predictors by comparing the magnitude of the coefficients output by models fitted with scaled and centered predictor variables, hereafter referred to as standardized estimate. Models were also fitted using unscaled inputs, so that coefficient values could be meaningfully interpreted and average marginal effects calculated. We calculated the average marginal effect as the difference in predicted probability of structure loss caused by a one unit change in the predictor averaged across all observed values of the predictors. Average marginal effects are always reported as change in percentage points (pp).

3. Results

3.1. Canopy segmentation

Our alignment of the satellite and LiDAR data resulted in and RMSE of 2.05 m and 2.08 m for the Eaton and Palisades fires respectively. Because our satellite data was not used to identify any features, but only to assess the NDVI of potential canopy polygons, this level of alignment was acceptable for our purpose. Our canopy segmentation process generated 25,895 canopy polygons inside the Eaton fire perimeter and 26,998 inside the Palisades fire perimeter. Canopy segmentation accuracy was 88%, with 86% sensitivity (true positive detection) and 90% specificity (true negative detection) for the Eaton fire canopy polygons. The Palisades canopy polygons had 88% accuracy, 88% sensitivity, and 87% specificity. For both fires, we correctly identified pixels as canopy or not canopy 88% of the time. Our process was similarly able to identify non-canopy pixels as canopy pixels (87–90% specificity vs. 86–88% sensitivity).

3.2. Spatial summary statistics

Our final study area for the Eaton fire was 9.84 km^2, containing 25,895 canopy polygons (canopy area 2.78 km^2) and 8965 structure footprints. The mean canopy density was 26.6 canopies/ha and the mean structure density was 14.2 structures/ha (Supp. Fig. 3). Within our study area, 7045 (79%) of the structures were classified as destroyed and 1920 structures (21%) were classified as not destroyed. The mean area of canopy within 2 m of a structure was 41.4 m^2. The mean distance to the nearest canopy from a structure was 1.25 m and the mean distance to the closest structure was 4.4 m. The mean wind direction was from the NE (52 °).

Our final study area for the Palisades fire was 7.42 km^2. It contained 26,998 canopy polygons (canopy area 2.11 km^2) and 6117 structure footprints. The mean canopy density was 34.6 canopies/ha and the mean structure density was 13.6 structures/ha (Supp. Fig. 4). Within our study area, 4655 (76%) of the structures were classified as destroyed and 1462 (24%) structures were classified as not destroyed. The mean area of canopy within 2 m of a structure was 46.7 m^2. The mean distance to the closest structure was 4.03 m. The mean wind direction from was from the NE (38 °)

3.2.1. Eaton fire

Structure density was the strongest predictor of structure loss in the Eaton fire, where structures in areas of higher structure density were more likely to be destroyed [average marginal effect (AME) 1.8 pp per structure/ha; Table 2, Fig. 3A, Fig. 4]. Structures were also more likely to be destroyed if there was less distance to the nearest structure (AME −0.47 pp per m) and had more structure footprint within 2 m of them (AME 0.31 pp per m^2; Table 2, Fig. 4). Canopy density was the second strongest predictor of structure loss in the Eaton fire (AME 0.6 pp per canopy/ha), where structures with more canopy density around them were slightly more likely to be destroyed. Similarly, structures with more canopy within 2 m of their perimeter were slightly more likely to be destroyed (AME 0.07 pp per m^2 of canopy). There was a significant interaction between canopy density and structure density, where structures in areas of higher canopy density were more likely to be destroyed, but the association was much stronger in areas of high structure density (Figs. 3A, 5A). Slope had a weak association with probability of structure loss, where structures on steeper slopes were more likely to be lost (AME 1.3 pp per deg.). We did not identify an association of wind direction or speed with structure loss, where neither the degrees from downwind of the nearest canopy or the nearest structure had a significant association with the probability of structure loss. The distance from a structure to the nearest canopy, elevation, and aspect also had no association with the probability of the structure being destroyed.

We estimated the effect of removing vegetation within 2 m of a structure by calculating the change in the probability of structure loss between the mean and the minimum values in our dataset for tree canopy area in zone zero. Structures with the mean canopy within 2 m of them (41.4 m^2) were 3.1 pp more likely to be destroyed than structures with the minimum (0 m^2) amount of canopy within 2 m of them.

3.2.2. Palisades fire

Structure density was also the strongest predictor of structure loss in the Palisades fire, where structures in areas of higher structure density were more likely to be destroyed (AME 1.5 pp per structure/ha; Table 2, Fig. 3B, Fig. 4). Structures were also more likely to be destroyed if there was less distance to the nearest structure (-0.20 pp per m). Average wind speed and elevation were the second and third strongest predictors of structure loss, where structures that experienced higher wind speeds on average (AME 4.0 pp per mph) and at lower elevations (AME −0.30 pp per m) were more likely to be destroyed. Canopy density was the fourth strongest predictor of structure loss (AME −0.20 pp per tree/ha), although in the opposite direction as Eaton, where structures with less canopy density around them were more likely to be destroyed in the Palisade fire. The interaction between structure density and canopy density was also significant in the Palisades fire, also in the opposite direction as Eaton, where canopy density had no association with structure loss in areas of low structure density (Figs. 3B, 5B). Structures were more likely to be destroyed if they were closer to the nearest canopy (AME 0.36 pp per m; Table 2, Fig. 4). The degrees from downwind of the nearest canopy, degrees from downwind of the nearest structure, slope, area of canopy within 2 m, and area of structure footprint within 2 m had no association with the probability of structure loss.

We also estimated the potential impact of removing vegetation within zone zero in the Palisades. Structures with the mean area of canopy within 2 m of them (46.7 m^2) were 1.0 percentage points more likely to be destroyed than structures with the minimum area (0 m^2) of canopy within 2 m of them.

4. Discussion

We examined 15,082 structures and 52,893 canopies within the Eaton and Palisades fire scars and evaluated the relative associations of urban canopy and structure density with structure damage. We found that structure density was by far the strongest predictor of structure loss, where structures in denser areas were more likely to be destroyed (Table 2, Fig. 3 & 4). The distance to the nearest structure also had a significant, yet smaller association with structure loss (Table 2, Fig. 3 &

Table 2
Estimates from models predicting structure loss. Variable importance was calculated using the absolute value of the standardized estimate. The average marginal effect (AME) is the difference in predicted probability of structure loss caused by a one unit change in the predictor averaged across all observed values of the other predictors. Asterisks indicate significance (*: t > 1.96, **: t > 2.6, ***: t > 3.3).

	Eaton			Palisades		
Predictor	Variable importance	Standardized estimate	AME	Variable importance	Standardized estimate	AME
Structure density (ha^{-1})	1	0.75858***	0.0184	1	1.00508***	0.0153
Canopy density (ha^{-1})	2	0.42023***	0.00597	4	-0.29224*	-0.00201
Area of canopy within 2 m (m^2)	3	0.2501***	0.000718	8	0.0943	0.000217
Canopy density x Structure density	4	0.22441***	NA	5	-0.2498**	NA
Elevation (m)	5	0.21058	0.00167	3	-0.44839**	-0.0029
Distance to nearest structure (m)	6	-0.18761***	-0.00471	7	-0.09646*	-0.00203
Area of structure footprint within 2 m (m^2)	7	0.11714**	0.00307	9	0.02122	0.000276
Slope (deg.)	8	0.09027*	0.0132	13	0.00204	0.000126
Mean wind spd. (mph)	9	0.05481	0.000302	12	0.00556	1.77e-05
Degs. from downwind of canopy	10	-0.04493	-0.000103	11	0.00677	1.28e-05
Distance to nearest canopy(m)	11	0.04381	0.00844	2	0.4621**	0.0405
Degs. from downwind of structure	12	-0.04138	-0.00144	6	-0.15744*	-0.0036
Aspect (deg.)	13	-0.03489	-8.13E-05	10	-0.0116	-1.84E-05

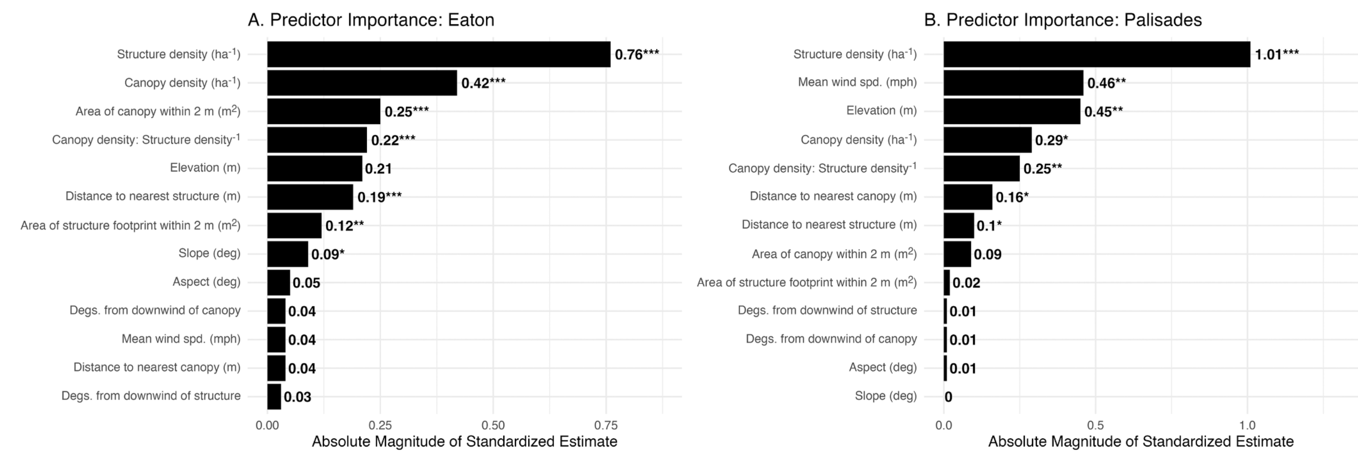

Fig. 3. Model predictor importance for the Eaton (A) and Palisades (B) fires. Bars show the value of the absolute magnitude of the standardized estimate for each predictor. Asterisks indicate significance (*: t > 1.96, **: t > 2.6, ***: t > 3.3).

4). These results align with previous findings that in urban conflagrations, the spacing between structures is the most significant factor associated with structure loss (Himoto and Tanaka, 2008; Syphard and Keeley, 2019; Troy et al., 2022; Zamanialaei et al., 2025).

In contrast, the association of urban canopy with structure loss was inconsistent with small effect sizes. For example, while canopy density was the second most important predictor of structure loss in both fires, it had opposite associations in the two fires (Table 2, Figs. 3–5). In the Eaton fire, structures in areas of higher canopy density were more likely to be lost, whereas in the Palisades fire, structures in areas of higher canopy density were less likely to be lost. This result suggests either correlation between canopy density and an unmeasured variable, or perhaps that in the Eaton fire, vegetation was more likely to burn and become an ember source, while in the Palisades fire, vegetation may have acted more as an ember catcher or buffer.

Further, in both fires, the association of canopy density with structure loss were highly dependent on structure density (Fig. 5). In the Eaton fire, the positive relationship between canopy density and structure loss was much stronger in areas of high structure density (Fig. 5A). Similarly in the Palisades, but in the opposite direction, the negative relationship between canopy density and structure loss was strong in areas of high structure density and non-existent in areas of low structure density (Fig. 5B). These results indicate that while urban canopy has some association with structure loss, this association is variable and depends largely on the spatial orientation of structures.

Without vegetation maintenance or health data, we can only speculate as to why canopy density had the opposite associations in the two fires. It is possible that vegetation in the Palisades fire had higher fuel moisture and less immediately combustible tissue due to differences in health, irrigation, pruning, species composition, or other factors (Boving et al., 2023; Huber-Smith et al., 2023; Possell and Bell, 2012). Future studies should investigate whether fuel moisture and species composition contribute to the association of canopy density with structure loss in urban conflagrations.

In the Eaton fire, having more canopy within 2 m of a structure slightly increased the probability of structure loss (Eaton: 0.07 pp per m^2). There are two primary mechanisms that might explain this association. One is that in some cases, vegetation ignited and created fuel continuity between structures. However, given that vegetation is saturated with water, widespread ignition seems unlikely. Another possible explanation is that structures with more canopy in proximity were more likely to have a significant accumulation of dry, ignitable litter on and around the structures (Barkeley et al., 2004). Notably, these fires occurred in January, when deciduous trees would have recently littered dry leaves that may not have been cleared in time for the fire. It would be useful to know if the effect of canopy within 2 m of a structure was greater for deciduous trees. Without tree inventory data from private property, we cannot yet address this question.

This result has implications for how zone zero policies should be implemented in urban areas, suggesting that perhaps litter maintenance and proper pruning could mitigate many of the potential impacts, rather than entire tree removal. A recent study examining the major contributors to structure loss in five major wildfires across California found that the amount of vegetation in zone zero was ranked fifth in importance

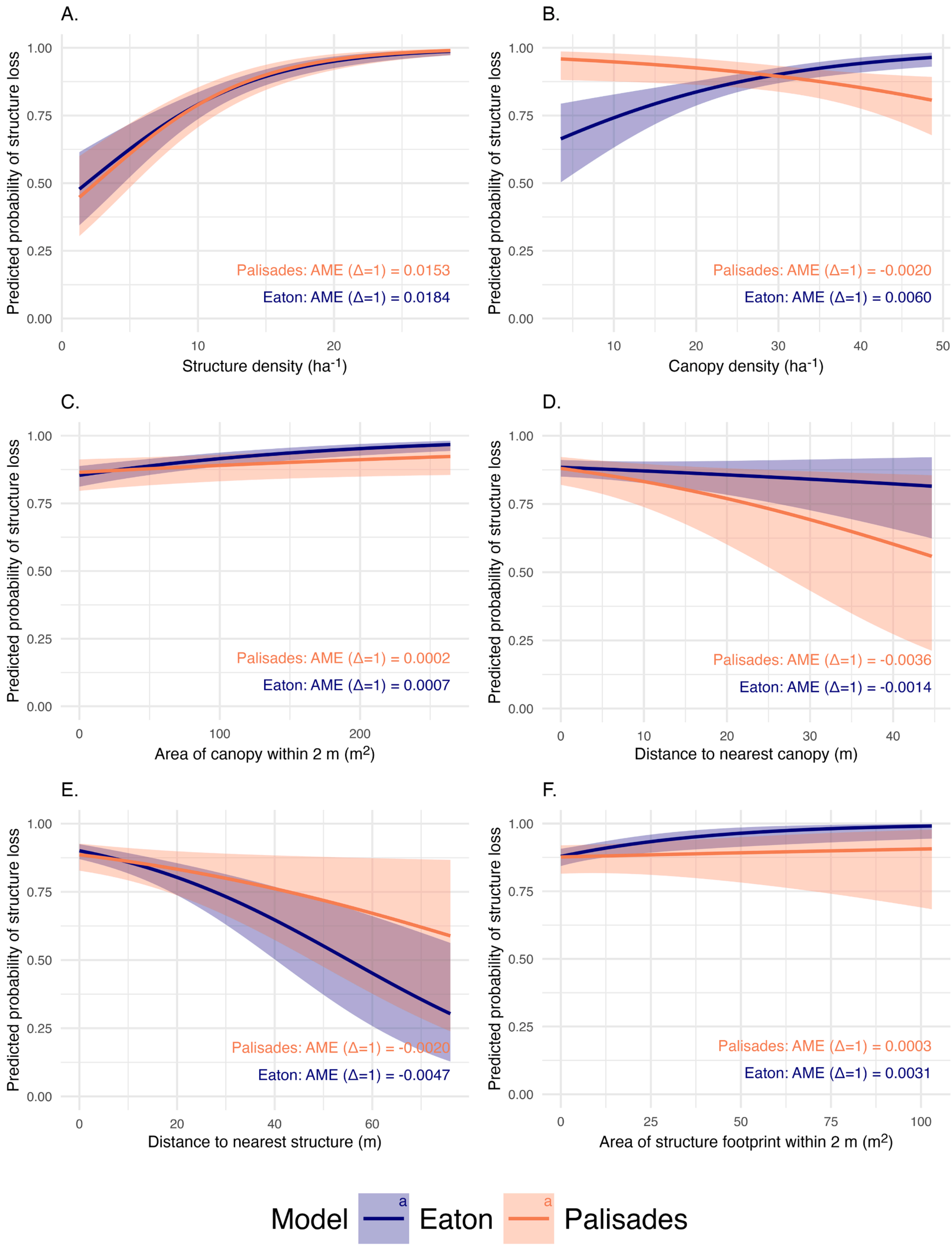

Fig. 4. Marginal change in predicted probability of structure loss across the range of the top predictors relating to the distribution of structures and vegetation in our two models. All other predictors were fixed at their mean values. Error bars represent prediction intervals. AME indicates the average marginal effect as change in probability of structure loss for a one unit change in the predictor.

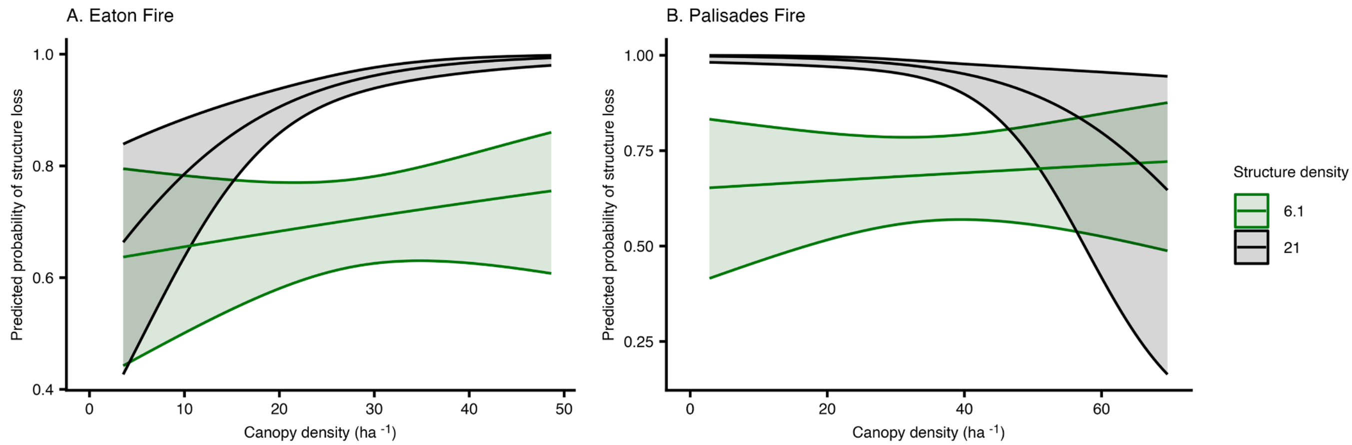

Fig. 5. Plot showing the predicted interaction between canopy and structure density in the Eaton fire (A) and the Palisades fire (B). 10th (green) and 90th (black) percent quantile values are shown for structure density to visualize the relationships. Lines are fitted values and shading shows the 95% prediction interval.

after structure density and home hardening measures (Zamanialaei et al., 2025). These results further reveal that structural fire hardening should be the primary focus of urban fire mitigation policies and efforts, and fire mitigation policies should weigh the negative impacts of canopy loss with the relatively minor association between vegetation and structure loss in urban fires.

In addition to the spatial distribution of urban vegetation and structures, there are other factors that affect the likelihood of structure loss, such as fire suppression, home hardening, and the behavior of fire itself (Quarles et al., 2010; Syphard and Keeley, 2019). To account for the effects of fire suppression, we excluded the area within 50 m of the fire perimeters from our study, as there may have been more fire suppression effort in those areas. Without data on home hardening characteristics or construction date, which is generally correlated with home hardening, we were unable to account for these well-established contributors to structure loss in urban conflagrations (Mockrin et al., 2023; Syphard and Keeley, 2019; Zamanialaei et al., 2025). Further, we did not have fire behavior data, nor were we able to simulate it, as relevant fire simulation models are not yet built for urban settings (Purnomo et al., 2024). However, our spatially explicit model inherently controls for variation in local fire intensity and spread patterns within each neighborhood and we tried to account for wind speed, direction, slope, aspect and elevation. There were some other sources of error that were difficult to quantify. We had 12% error in our canopy delineation, however this should be randomly distributed relative to the likelihood of home loss and so we did not explicitly incorporate this into our models. There may also have been some error introduced by changes in the study areas after our data was generated, such as structures built after 2020, or trees removed after 2023. Again there is no reason to expect these factors to correlate with the probability of structure loss and we do not expect that they introduced bias into our models. Future efforts should focus on incorporating the known predictors of structure loss referenced above and comparing their effects to those of urban trees.

5. Conclusion

Our results have major implications on urban forest management, demonstrating that the spatial distribution of buildings is far more important than the spatial distribution of urban canopy. Future research should account for the effects of irrigation, tree and roof maintenance, species-specific flammability, and home hardening when examining the association of urban canopy with structure loss in fires. The minor and inconsistent association of vegetation and structure loss in urban conflagrations requires further study before implementing policies that remove valuable urban canopy.

Declaration of generative AI and AI-assisted technologies in the manuscript preparation process

During the preparation of this work the authors used ChatGPT to generate first drafts of code and verify that inline citations matched the works cited. After using this tool, the authors reviewed and edited the content as needed and take full responsibility for the content of the published article.

Funding

This work was supported in part by a generous donation from Jack Dangermond and ESRI.

CRediT authorship contribution statement

Reed Kenny: Writing – review & editing, Writing – original draft, Software, Methodology, Conceptualization. **Camille Pawlak:** Writing – review & editing, Methodology, Conceptualization. **Jason Johns:** Writing – review & editing, Methodology, Conceptualization. **Jenn Yost:** Writing – review & editing, Methodology, Conceptualization. **Andrew Fricker:** Writing – review & editing, Methodology, Conceptualization. **Matt Ritter:** Writing – review & editing, Methodology, Funding acquisition, Conceptualization.

Declaration of Competing Interest

The authors declare that they have no known competing financial interests or personal relationships that could have appeared to influence the work reported in this paper.

Acknowledgements

We thank Caroline Kelleher, Brian Dukes, Alex Lung, Lena Rasch, Adam Segal, Collin Parker, Elena Wilkinson, Ella Hood, Isabella Paz, Kyle Mahon, Savannah Bosley and Aakash Ahamed for assistance digitizing tree canopies. We thank two anonymous reviewers for comments that improved the manuscript.

Appendix A. Supporting information

Supplementary data associated with this article can be found in the online version at doi:10.1016/j.ufug.2026.129470.

References

Abatzoglou, J.T., Battisti, D.S., Williams, A.P., Hansen, W.D., Harvey, B.J., Kolden, C.A., 2021. Projected increases in western us forest fire despite growing fuel constraints. Commun. Earth & Environ. 2 (1), 227. https://doi.org/10.1038/s43247-021-00299-0.

Barkeley, Y.C., Schnepf, C., Cohen, J.D., 2004. Protecting and landscaping homes in the wildland/urban interface. Station Bulletin #67, January 2005. Idaho Forest, Wildlife and Range Experiment Station. University of Idaho Extension, *Moscow, ID*, p. *21*. ⟨https://research.fs.usda.gov/treesearch/22257⟩ (p.).

Bijoor, N.S., McCarthy, H.R., Zhang, D., Pataki, D.E., 2012. Water sources of urban trees in the los angeles metropolitan area. Urban Ecosyst. 15 (1), 195–214. https://doi.org/10.1007/s11252-011-0196-1.

Boving, I., Celebrezze, J., Salladay, R., Ramirez, A., Anderegg, L.D.L., Moritz, M., 2023. Live fuel moisture and water potential exhibit differing relationships with leaf-level flammability thresholds. Funct. Ecol. 37 (11), 2770–2785. https://doi.org/10.1111/1365-2435.14423.

Brigham, C., Scott, C., Anderson, S.W., Phan, M., Arrowsmith, R., Nandigam, V., et al., 2024. Improving error analysis in topographic differencing via an on-demand tool. AGU. ⟨https://agu.confex.com/agu/agu24/meetingapp.cgi/Paper/1694264⟩.

CalFire, 2025. Defensible space - zones 0. 1 & 2. Defensible Space - Zones 0 1 & 2. ⟨https://calfire-umb05.azurewebsites.net/projects-and-programs/defensible-space-zones-0-1-2/⟩ (accessed 2025-07-18).

County of Los Angeles, 2025. Los Angeles region imagery acquisition consortium data. ⟨https://lariac-lacounty.hub.arcgis.com/⟩.

Dalponte, M., Coomes, D.A., 2016. Tree-centric mapping of forest carbon density from airborne laser scanning and hyperspectral data. Methods Ecol. Evol. 7 (10), 1236–1245. https://doi.org/10.1111/2041-210X.12575.

Davies, Z.G., Edmondson, J.L., Heinemeyer, A., Leake, J.R., Gaston, K.J., 2011. Mapping an urban ecosystem service: quantifying above-ground carbon storage at a city-wide scale. J. Appl. Ecol. 48 (5), 1125–1134. https://doi.org/10.1111/j.1365-2664.2011.02021.x.

Dowell, D.C., Alexander, C.R., James, E.P., Weygandt, S.S., Benjamin, S.G., Manikin, G. S., et al., 2022. The high-resolution rapid refresh (hrrr): an hourly updating convection-allowing forecast model. part i: motivation and system description. Weather Forecast. 37 (8), 1371–1395. https://doi.org/10.1175/WAF-D-21-0151.1.

Ehleringer, J.R., Dawson, T.E., 1992. Water uptake by plants: perspectives from stable isotope composition. Plant Cell & Environ. 15 (9), 1073–1082. https://doi.org/10.1111/j.1365-3040.1992.tb01657.x.

Escobedo, F.J., Yadav, K., Ossola, A., Klein, R., Drury, S., 2024. Urban forest cover and ecosystem service response to fire varies across California communities. Urban For. & Urban Green. 101, 128547. https://doi.org/10.1016/j.ufug.2024.128547.

Filkov, A.I., Tihay-Felicelli, V., Masoudvaziri, N., Rush, D., Valencia, A., Wang, Y., et al., 2023. A review of thermal exposure and fire spread mechanisms in large outdoor fires and the built environment. Fire Saf. J. 140, 103871. https://doi.org/10.1016/j.firesaf.2023.103871.

Giacinto, J.J., Fricker, G.A., Ritter, M., Yost, J., Doremus, J., 2021. Urban forest biodiversity and cardiovascular disease: potential health benefits from California's street trees. PLOS ONE 16 (11), e0254973. https://doi.org/10.1371/journal.pone.0254973.

Guirguis, K., Hatchett, B., Clemesha, R., Aguilera, R., Gershunov, A., Campbell, I., et al., 2025. Compound atmospheric drivers of the catastrophic 2025 los angeles urban firestorm. npj Nat. Hazards 2 (1), 103. https://doi.org/10.1038/s44304-025-00155-7.

Hardy, C.C., Burgan, R.E., 1999. Evaluation of NDVI for monitoring live moisture in three vegetation types of the western U. S. Photogramm. Eng. & Remote Sens. 65 (5).

Hijmans, R., 2025. Rspatial/Terra. ⟨https://github.com/rspatial/terra⟩.

Himoto, K., Tanaka, T., 2008. Development and validation of a physics-based urban fire spread model. Fire Saf. J. 43 (7), 477–494. https://doi.org/10.1016/j.firesaf.2007.12.008.

Huber-Smith, N.K., Morley, E.S., Krix, D.W., Murray, M.L., Webb, J.K., Martin, L.J., et al., 2023. Shoot flammability patterns in native and exotic street tree species at the wildland–urban interface of eastern Australia. Fire 6 (11), 440. https://doi.org/10.3390/fire6110440.

Knapp, E.E., Valachovic, Y.S., Quarles, S.L., Johnson, N.G., 2021. Housing arrangement and vegetation factors associated with single-family home survival in the 2018 Camp fire, California. Fire Ecol. 17 (1), 25. https://doi.org/10.1186/s42408-021-00117-0.

Kuhn, M., 2008. Building predictive models in r using the caret package. J. Stat. Softw. 28, 1–26. https://doi.org/10.18637/jss.v028.i05.

LA County DRP GIS Section, 2025. Zone 0 - Potential Impacts. ⟨https://experience.arcgis.com/experience/d9cdf20067544c65a6339254098f7f44/page/Home⟩.

LA Internal Services Department, 2020. Countywide building outlines (2020). *LA GeoHub*. ⟨https://geohub.lacity.org/maps/e6a1e375e12a4fe6849d896a26ec028a/about⟩ (accessed 2025-09-26).

Lindgren, F., Rue, H., Lindström, J., 2011. An explicit link between gaussian fields and gaussian Markov random fields: the stochastic partial differential equation approach. J. R. Stat. Soc. Ser. B Stat. Methodol. 73 (4), 423–498. https://doi.org/10.1111/j.1467-9868.2011.00777.x.

Mockrin, M.H., Locke, D.H., Syphard, A.D., O'Neil-Dunne, J., 2023. Using high-resolution land cover data to assess structure loss in the 2018 Woolsey fire in southern California. J. Environ. Manag. 347, 118960. https://doi.org/10.1016/j.jenvman.2023.118960.

National Interagency Fire Perimeters, 2025. Current interagency wildfire perimeters. ⟨https://data-nifc.opendata.arcgis.com/datasets/nifc::wfigs-current-interagency-fire-perimeters/about⟩.

Nowicki, B., 2002. The community protection zone: defending houses and communities from the threat of forest fire. Cent. Biol. Divers. ⟨https://www.biologicaldiversity.org/publications/papers/wui1.pdf⟩.

Pataki, D.E., Alberti, M., Cadenasso, M.L., Felson, A.J., McDonnell, M.J., Pincetl, S., et al., 2021. The benefits and limits of urban tree planting for environmental and human health. Front. Ecol. Evol. 9. https://doi.org/10.3389/fevo.2021.603757.

Pebesma, E., Bivand, R., 2023. Spatial data science: with applications in r. Chapman and Hall/CRC, New York. https://doi.org/10.1201/9780429459016.

Peduzzi, P., Concato, J., Kemper, E., Holford, T.R., Feinstein, A.R., 1996. A simulation study of the number of events per variable in logistic regression analysis. J. Clin. Epidemiol. 49 (12), 1373–1379. https://doi.org/10.1016/s0895-4356(96)00236-3.

Penman, S.H., Price, O.F., Penman, T.D., Bradstock, R.A., 2019. The role of defensible space on the likelihood of house impact from wildfires in forested landscapes of south eastern Australia. Int. J. Wildland Fire 28 (1), 4–14. https://doi.org/10.1071/WF18046.

Possell, M., Bell, T.L., 2012. The influence of fuel moisture content on the combustion of Eucalyptus foliage. Int. J. Wildland Fire 22 (3), 343–352. https://doi.org/10.1071/WF12077.

Price, O., Ondei, S., Bowman, D.M.J.S., 2025. Progress and prospects for predicting wildfire spread through the wildland-urban interface. Int. J. Disaster Risk Reduct. 121, 105392. https://doi.org/10.1016/j.ijdrr.2025.105392.

Price, O.F., Bradstock, R.A., 2013. The spatial domain of wildfire risk and response in the wildland urban interface in Sydney, Australia. Nat. Hazards Earth Syst. Sci. 13 (12), 3385–3393. https://doi.org/10.5194/nhess-13-3385-2013.

Purnomo, D.M.J., Qin, Y., Theodori, M., Zamanialaei, M., Lautenberger, C., Trouvé, A., et al., 2024. Reconstructing modes of destruction in wildland–urban interface fires using a semi-physical level-set model. Proc. Combust. Inst. 40 (1), 105755. https://doi.org/10.1016/j.proci.2024.105755.

Quarles, S.L., Valachovic, Y., Nakamura, G.M., Nader, G.A., De Lasaux, M.J., 2010. Home survival in wildfire-prone areas: building materials and design considerations. University of California, Agriculture and Natural Resources. https://doi.org/10.3733/ucanr.8393.

Riley, R.D., Snell, K.I., Ensor, J., Burke, D.L., Harrell Jr, F.E., Moons, K.G., et al., 2019. Minimum sample size for developing a multivariable prediction model: part ii - binary and time-to-event outcomes. Stat. Med. 38 (7), 1276–1296. https://doi.org/10.1002/sim.7992.

Roussel, J.-R., Auty, D., Coops, N.C., Tompalski, P., Goodbody, T.R.H., Meador, A.S., et al., 2020. LidR: an r package for analysis of airborne laser scanning (als) data. Remote Sens. Environ. 251, 112061. https://doi.org/10.1016/j.rse.2020.112061.

Rousset, F., Ferdy, J.-B., 2014. Testing environmental and genetic effects in the presence of spatial autocorrelation. Ecography 37 (8), 711–813. https://doi.org/10.1111/ecog.00566.

Speak, A.F., Salbitano, F., 2023. The impact of pruning and mortality on urban tree canopy volume. Urban For. & Urban Green. 79, 127810. https://doi.org/10.1016/j.ufug.2022.127810.

Syphard, A.D., Keeley, J.E., 2019. Factors associated with structure loss in the 2013–2018 California wildfires. Fire 2 (3), 49. https://doi.org/10.3390/fire2030049.

Syphard, A.D., Keeley, J.E., 2020. Why are so many structures burning in California. Fremontia 47 (2), 28–25.

Syphard, A.D., Keeley, J.E., Gough, M., Lazarz, M., Rogan, J., 2022. What makes wildfires destructive in california? Fire 5 (5), 133. https://doi.org/10.3390/fire5050133.

Troy, A., Moghaddas, J., Schmidt, D., Romsos, J.S., Sapsis, D.B., Brewer, W., et al., 2022. An analysis of factors influencing structure loss resulting from the 2018 Camp fire. Int. J. Wildland Fire 31 (6), 586–598. https://doi.org/10.1071/WF21176.

Van Der Walt, S., Schönberger, J.L., Nunez-Iglesias, J., Boulogne, F., Warner, J.D., Yager, N., et al., 2014. Scikit-image: image processing in python. PeerJ 2, e453. https://doi.org/10.7717/peerj.453.

Wagenbrenner, N., Shannon, K., tfinney9, latwood, Forthofer, J., RuiyuZhang, S.D., et al., 2024. Firelab/Wind. 3 (11), 2. https://doi.org/10.5281/ZENODO.14157304.

Wang, D., Guan, D., Zhu, S., Kinnon, M.M., Geng, G., Zhang, Q., et al., 2021. Economic footprint of California wildfires in 2018. Nat. Sustain. 4 (3), 252–260. https://doi.org/10.1038/s41893-020-00646-7.

Zamanialaei, M., San Martin, D., Theodori, M., Purnomo, D.M.J., Tohidi, A., Lautenberger, C., et al., 2025. Fire risk to structures in California's wildland-urban interface. Nat. Commun. 16 (1), 8041. https://doi.org/10.1038/s41467-025-63386-2.

Zhang, D., Yao, M., Chen, Y., Liu, Y., 2025. The role of urban vegetation in mitigating fire risk under climate change: a review. Sustainability 17 (6), 2680. https://doi.org/10.3390/su17062680.